

Short Communication

## Intermediate Temperature Electrochemical Properties of Al<sup>3+</sup> and K<sup>+</sup> Double Doped Strontium Silicate

Wei Chen<sup>1</sup>, Wenli Hu<sup>1</sup>, Hongtao Wang<sup>1,2\*</sup>

<sup>1</sup> Fuyang Preschool Education College, Fuyang 236015, China;

<sup>2</sup> School of Chemical and Material Engineering, Fuyang Normal University, Fuyang 236037, China

\*E-mail: [hongtaoking3@163.com](mailto:hongtaoking3@163.com), [hwang@fync.edu.cn](mailto:hwang@fync.edu.cn)

Received: 2 June 2019 / Accepted: 8 July 2019 / Published: 5 August 2019

In this study, K<sup>+</sup> and Al<sup>3+</sup> double doped strontium silicate was synthesized via a solid state reaction method using strontium carbonate, silicon dioxide, potassium carbonate and aluminum trioxide as raw materials. Intermediate temperature conductivities and fuel cell properties of Sr<sub>0.6</sub>K<sub>0.4</sub>Si<sub>0.9</sub>Al<sub>0.1</sub>O<sub>3-α</sub> electrolyte were studied. X-ray diffractions of Sr<sub>0.6</sub>K<sub>0.4</sub>SiO<sub>3-α</sub> and Sr<sub>0.6</sub>K<sub>0.4</sub>Si<sub>0.9</sub>Al<sub>0.1</sub>O<sub>3-α</sub> results showed that the second phase of K<sub>2</sub>Si<sub>2</sub>O<sub>5</sub> can be effectively inhibited when two metal oxides are doped. The relation between conductivity and temperature of the samples indicated that the curves agreed well with the Arrhenius formula. Sr<sub>0.6</sub>K<sub>0.4</sub>Si<sub>0.9</sub>Al<sub>0.1</sub>O<sub>3-α</sub> showed the highest maximum power density of 44.2 mW·cm<sup>-2</sup> at 800 °C.

**Keywords:** Electrolyte; SrSiO<sub>3</sub>; Fuel cell; Conductivity; XRD

### 1. INTRODUCTION

Solid electrolytes have been extensively investigated in solid oxide fuel cells (SOFCs), gas sensors etc [1-7]. Oxygen-ion solid electrolytes, such as CeO<sub>2</sub> and ZrO<sub>2</sub>-based conductors, usually require a high operating temperature (800–1000 °C) which limits their application. Therefore, searching for new types of electrolyte for application at medium temperature (400–800 °C) has become a research hotspot [8-11].

Recently, Goodenough et al. [12-14] reported new oxide-ion electrolytes of sodium or potassium doped strontium silicate which had excellent intermediate temperature electrochemical properties. In a series of papers [12-14], the solid solution of Sr<sub>1-x</sub>M<sub>x</sub>SiO<sub>3-α</sub> (M = Na<sup>+</sup>, K<sup>+</sup>) was 45% and exhibited the highest conductivity > 0.1 S·cm<sup>-1</sup> at intermediate temperature. Meng et al. [15] synthesized Sr<sub>1-x</sub>Na<sub>x</sub>SiO<sub>3-x/2</sub> (x = 0.2, 0.3, 0.4, 0.45) electrolytes using a spark plasma sintering method at the low temperature of 850 °C. Ramamurthy et al. [16] studied electrochemical properties of Sr<sub>1-x</sub>K<sub>x</sub>SiO<sub>3-α</sub> and

found amorphous  $K_2Si_2O_5$  existed between grain boundaries. The structural and conduction mechanisms of doped strontium silicates were also discussed [17-23]. However, the reported  $SrSiO_3$  was doped with a single metal ion. There are no studies about bimetallic ion-doped  $SrSiO_3$ .

Therefore, in this study, aluminum and potassium double doped strontium silicate was synthesized due to the ionic radius of  $K^+$  and  $Al^{3+}$  being close to  $Sr^{2+}$  and  $Si^{4+}$ , correspondingly [24]. Intermediate temperature conductivities and fuel cell properties of  $Sr_{0.6}K_{0.4}Si_{0.9}Al_{0.1}O_{3-\alpha}$  electrolyte were also studied.

## 2. EXPERIMENTAL

$K^+$  and  $Al^{3+}$  double doped strontium silicate was synthesized via a solid state reaction method using strontium carbonate (8.8578 g), silicon dioxide (6.0084 g), potassium carbonate (2.7642g) and aluminum trioxide (0.5098 g) as raw materials. After weighing the above raw materials, they were put into a grinding bowl to make the mixture uniform. The grinding powders were pressed into pellets under 200MPa and calcined in a high temperature box furnace for 12 h at 950 °C and then 1000°C. For comparison,  $Sr_{0.6}K_{0.4}SiO_{3-\alpha}$  was also synthesized.

X-ray diffractions of  $Sr_{0.6}K_{0.4}SiO_{3-\alpha}$  and  $Sr_{0.6}K_{0.4}Si_{0.9}Al_{0.1}O_{3-\alpha}$  were measured in the scanning range from 10° to 70°. The surface and cross-section morphologies of  $Sr_{0.6}K_{0.4}SiO_{3-\alpha}$  and  $Sr_{0.6}K_{0.4}Si_{0.9}Al_{0.1}O_{3-\alpha}$  were observed by scanning electron microscopy (SEM).

For impedance measurements, the slices were ground to 1.0 mm with 1000-1200 meshes of fine sandpaper. The polished slice had a circle of 8 mm (area: 0.5 cm<sup>2</sup>) in diameter in the center and painted Pd-Ag paste. The glass was used to seal the ceramic pipes. After testing air tightness, the sample was connected to the electrochemical workstation (CHI660E). The impedance measurements were tested using the A.C. impedance method in a three-electrode mode from 0.1 Hz to 1 MHz frequency in dry nitrogen at 400-800 °C. At 800 °C, oxygen and hydrogen were introduced into the upper and lower gas chambers of the sample, respectively, and the  $H_2/O_2$  fuel cells were tested.

## 3. RESULTS AND DISCUSSION

X-ray diffractions of  $Sr_{0.6}K_{0.4}SiO_{3-\alpha}$  and  $Sr_{0.6}K_{0.4}Si_{0.9}Al_{0.1}O_{3-\alpha}$  were measured in the scanning range from 10° to 70° and are shown in Fig. 1. It is clear that  $Sr_{0.6}K_{0.4}Si_{0.9}Al_{0.1}O_{3-\alpha}$  electrolyte conforms to a single monoclinic crystal structure. It is noted that there are hetero-peaks in the  $Sr_{0.6}K_{0.4}SiO_{3-\alpha}$  sample, which are consistent with the  $K_2Si_2O_5$ . This indicates that the second phase of  $K_2Si_2O_5$  is produced when the potassium content is high. This is consistent with other reported results [16,18]. This indicates that the formation of the second phase can be effectively inhibited when two metal oxides are doped.

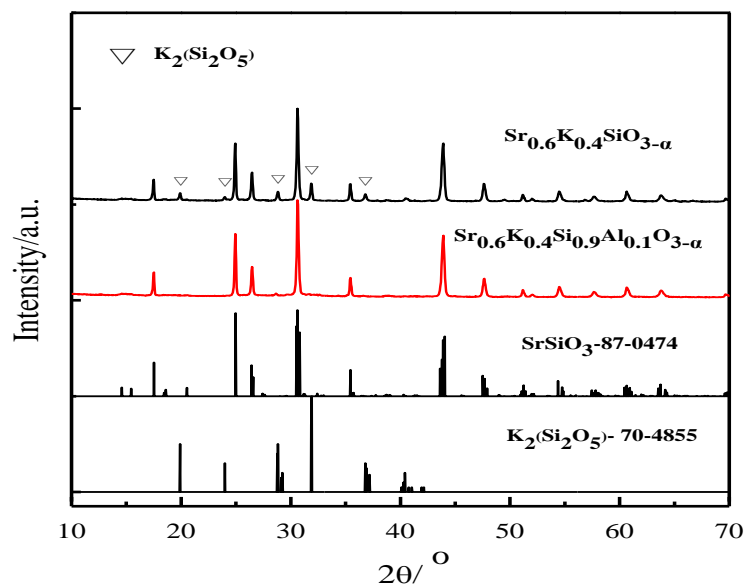


Figure 1. XRD patterns of  $\text{Sr}_{0.6}\text{K}_{0.4}\text{SiO}_{3-\alpha}$  and  $\text{Sr}_{0.6}\text{K}_{0.4}\text{Si}_{0.9}\text{Al}_{0.1}\text{O}_{3-\alpha}$ .

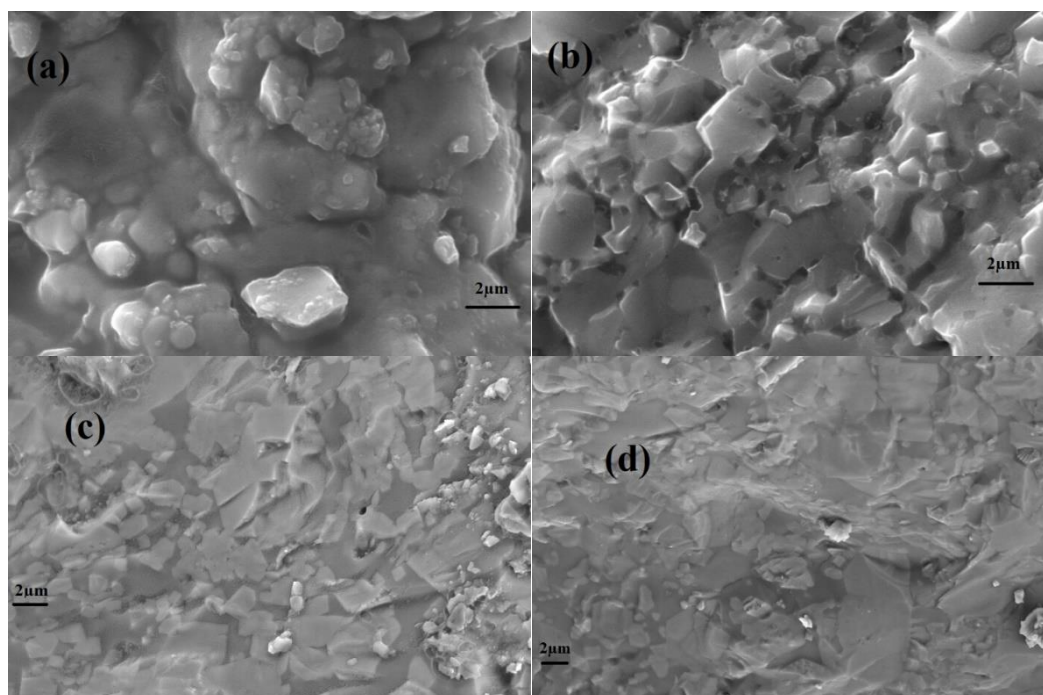
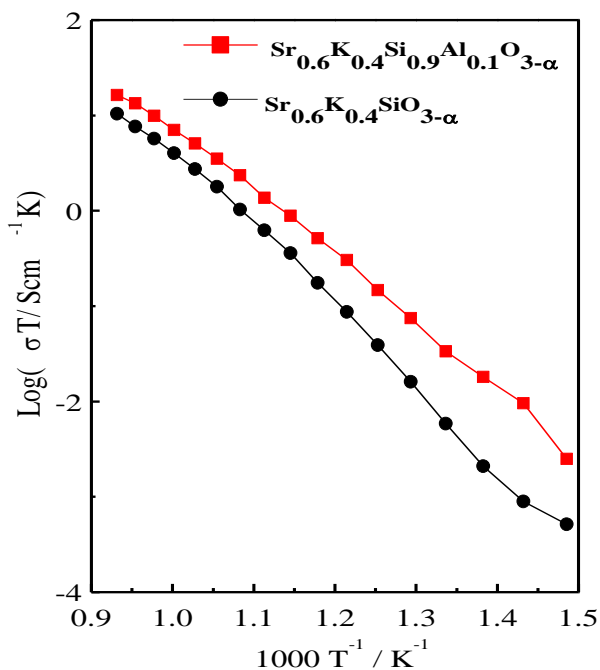


Figure 2. The surface and cross-section morphologies of  $\text{Sr}_{0.6}\text{K}_{0.4}\text{SiO}_{3-\alpha}$  (a,b) and  $\text{Sr}_{0.6}\text{K}_{0.4}\text{Si}_{0.9}\text{Al}_{0.1}\text{O}_{3-\alpha}$  (c,d).

The surface and cross-section SEM photos of  $\text{Sr}_{0.6}\text{K}_{0.4}\text{SiO}_{3-\alpha}$  and  $\text{Sr}_{0.6}\text{K}_{0.4}\text{Si}_{0.9}\text{Al}_{0.1}\text{O}_{3-\alpha}$  are displayed in Fig. 2. From Fig. 2,  $\text{Sr}_{0.6}\text{K}_{0.4}\text{SiO}_{3-\alpha}$  and  $\text{Sr}_{0.6}\text{K}_{0.4}\text{Si}_{0.9}\text{Al}_{0.1}\text{O}_{3-\alpha}$  are sintered well, with uniform properties, good compactness and high density, which could meet the measurement requirements of electrical properties. It can be seen that the bonding between grains is compact and there are no holes in the grains.



**Figure 3.** The relations between conductivity and temperature of  $\text{Sr}_{0.6}\text{K}_{0.4}\text{SiO}_{3-\alpha}$  and  $\text{Sr}_{0.6}\text{K}_{0.4}\text{Si}_{0.9}\text{Al}_{0.1}\text{O}_{3-\alpha}$  in dry nitrogen at 400-800 °C.

The relations between conductivity and temperature of  $\text{Sr}_{0.6}\text{K}_{0.4}\text{SiO}_{3-\alpha}$  and  $\text{Sr}_{0.6}\text{K}_{0.4}\text{Si}_{0.9}\text{Al}_{0.1}\text{O}_{3-\alpha}$  in dry nitrogen at 400-800 °C are displayed in Fig. 3. According to the impedance spectrogram of the sample, the change of conductivity with temperature was obtained.

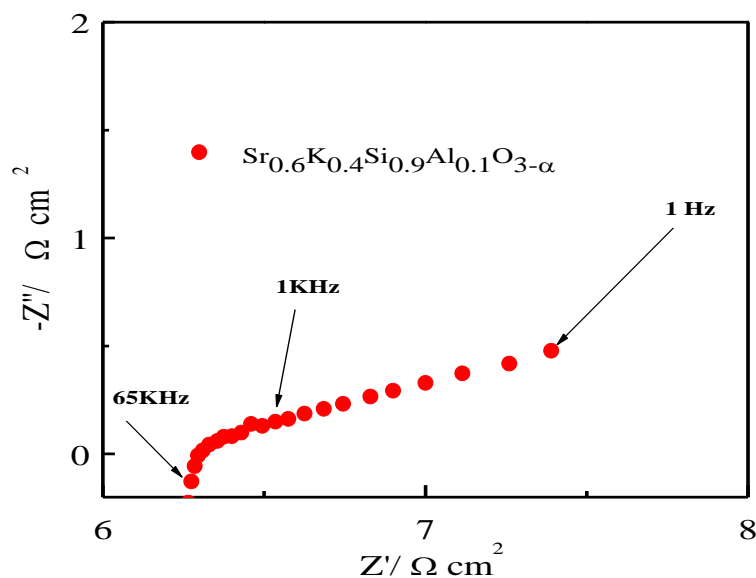


**Figure 4.** The electrochemical impedance spectroscopy (EIS) of  $\text{Sr}_{0.6}\text{K}_{0.4}\text{Si}_{0.9}\text{Al}_{0.1}\text{O}_{3-\alpha}$  under open circuit condition at 800 °C.

From Fig. 3, it can be clearly seen that the experimental data fit well with the straight line in the whole measuring temperature range, indicating that the conductivities agree with the Arrhenius formula. The conductivity of  $\text{Sr}_{0.6}\text{K}_{0.4}\text{Si}_{0.9}\text{Al}_{0.1}\text{O}_{3-\alpha}$  ( $1.2 \times 10^{-2} \text{ S} \cdot \text{cm}^{-1}$ ) is higher than that of  $\text{Sr}_{0.6}\text{K}_{0.4}\text{SiO}_{3-\alpha}$  ( $1.0 \times 10^{-2} \text{ S} \cdot \text{cm}^{-1}$ ) at  $800^\circ\text{C}$ . This indicates that the formation of the second phase  $\text{K}_2\text{Si}_2\text{O}_5$  in  $\text{Sr}_{0.6}\text{K}_{0.4}\text{SiO}_{3-\alpha}$  sample inhibits the growth of conductivity, while the formation of single phase can be maintained when  $\text{SrSiO}_3$  is double doped, thus promoting the increase of conductivity [16,22-23].

The EIS of typical SOFC electrolytes are composed of semicircles and rays. The semicircles in the low frequency region represent the internal impedance of grains, and the rays in the high frequency region represent the impedance of grain boundaries [16-20]. Fig. 4 is an impedance spectrogram of  $\text{Sr}_{0.6}\text{K}_{0.4}\text{Si}_{0.9}\text{Al}_{0.1}\text{O}_{3-\alpha}$  measured at  $800^\circ\text{C}$  under open circuit condition. The semicircle in the low frequency region shows the grain conduction in the sample, and it can be clearly seen that the semicircle and the ray overlap, which shows that the sample has good conductivity. The total resistance of  $\text{Sr}_{0.6}\text{K}_{0.4}\text{Si}_{0.9}\text{Al}_{0.1}\text{O}_{3-\alpha}$  is  $6.3 \Omega \cdot \text{cm}^2$  under open circuit condition at  $800^\circ\text{C}$ .

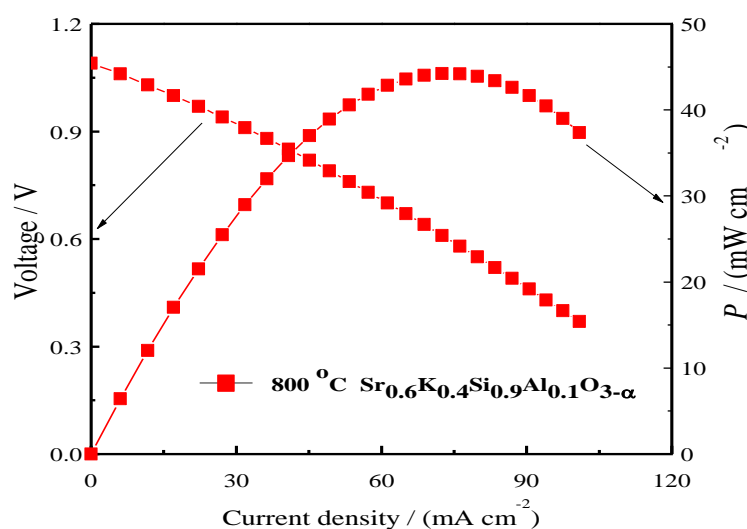


**Figure 5.** The fuel cell output curves using  $\text{Sr}_{0.6}\text{K}_{0.4}\text{Si}_{0.9}\text{Al}_{0.1}\text{O}_{3-\alpha}$  as electrolyte at  $800^\circ\text{C}$ .

Fig. 5 shows the fuel cell output curves of  $\text{Sr}_{0.6}\text{K}_{0.4}\text{Si}_{0.9}\text{Al}_{0.1}\text{O}_{3-\alpha}$  at  $800^\circ\text{C}$ . As can be seen from Fig. 5, the open circuit voltage (OCV) is 1.09 V, which indicates the sample is dense. With the decrease of open circuit voltage, the current and power density increase. When the open circuit voltage is 0.61 V, the highest current and power density are  $72.5 \text{ mA} \cdot \text{cm}^{-2}$  and  $44.2 \text{ mW} \cdot \text{cm}^{-2}$ , respectively.

#### 4. CONCLUSIONS

In this study,  $\text{Sr}_{0.6}\text{K}_{0.4}\text{SiO}_{3-\alpha}$  and  $\text{Sr}_{0.6}\text{K}_{0.4}\text{Si}_{0.9}\text{Al}_{0.1}\text{O}_{3-\alpha}$  were synthesized via a solid state reaction method using strontium carbonate, silicon dioxide, potassium carbonate and aluminum trioxide as raw materials. SEM photos showed that  $\text{Sr}_{0.6}\text{K}_{0.4}\text{SiO}_{3-\alpha}$  and  $\text{Sr}_{0.6}\text{K}_{0.4}\text{Si}_{0.9}\text{Al}_{0.1}\text{O}_{3-\alpha}$  were sintered well, with uniform properties, good compactness and high density. The conductivities of  $\text{Sr}_{0.6}\text{K}_{0.4}\text{SiO}_{3-\alpha}$  and  $\text{Sr}_{0.6}\text{K}_{0.4}\text{Si}_{0.9}\text{Al}_{0.1}\text{O}_{3-\alpha}$  were  $1.0 \times 10^{-2} \text{ S} \cdot \text{cm}^{-1}$  and  $1.2 \times 10^{-2} \text{ S} \cdot \text{cm}^{-1}$  in dry nitrogen at  $800^\circ\text{C}$ , respectively.

When the open circuit voltage was 0.61V, the highest current and power density of  $\text{Sr}_{0.6}\text{K}_{0.4}\text{Si}_{0.9}\text{Al}_{0.1}\text{O}_{3-\alpha}$  were  $72.5 \text{ mA}\cdot\text{cm}^{-2}$  and  $44.2 \text{ mW}\cdot\text{cm}^{-2}$  at  $800 \text{ }^\circ\text{C}$ , respectively.

#### ACKNOWLEDGEMENTS

This work was supported by the National Natural Science Foundation (No. 51402052) of China, the Natural Science Foundation of Higher Education Institutions in Anhui Province (No. KJ2019A1273, KJ2018A0980), Excellent Youth Foundation of Anhui Educational Committee (No. gxyq2018046), Horizontal cooperation project of Fuyang municipal government and Fuyang Normal College (No. HX2019004000, XDHXTD201704).

#### References

1. G. L. Liu, W. Liu Q. Kou and S. J. Xiao, *Int. J. Electrochem. Sci.*, 13 (2018) 2641.
2. Y. Yang, H. Hao, L. Zhang, C. Chen, Z. Luo, Z. Liu, Z. Yao, M. Cao and H. Liu, *Ceram. Int.*, 44 (2018) 11109.
3. S. Lee, and X. Guan, *MRS Communications*, 7 (2017) 199.
4. C. Xia, Z. Qiao, C. Feng, J. Kim, B. Wang and B. Zhu, *Materials*, 11(2018) 40.
5. Y. Tian, Z. Lü, X. Guo and P. Wu, *Int. J. Electrochem. Sci.*, 14 (2019) 1093.
6. H.-S. Kim, H.B. Bae, W.C. Jung and S.-Y. Chung, *Nano. Lett.*, 18(2018) 1110.
7. Z. Gong, W. Sun, Z. Jin, L. Miao and W. Liu, *ACS Appl. Energy Mater.*, 1(2018) 3521.
8. N. Zeeshan, Rafiuddin, *J. Adv. Res.*, 9 (2018) 35.
9. X. Fang, J. Zhu and Z. Lin, *Energies*, 11 (2018) 1735.
10. S. AjithKumar, P. Kuppasami and P. Vengatesh, *Ceram. Int.*, 44 (2018) 21188.
11. Y. Wan, B. He, R. Wang, Y. Ling and L. Zhao, *J. Power Sources*, 347 (2017) 14.
12. P. Singh and J.B. Goodenough, *Energy Environ. Sci.*, 5 (2012) 9626.
13. P. Singh and J.B. Goodenough, *J. Am. Ceram. Soc.*, 135 (2013) 10149.
14. T. Wei, P. Singh, Y. Gong, J.B. Goodenough, Y. Huang and K. Huang, *Energy Environ. Sci.*, 7 (2014) 1680.
15. F. Yang, Z. Yu, B. Meng, Y.J. Zhu, Q.Q. Yang, Z.L. Lin, H.M. Zhou and X. L. Liang, *Ionics* 22 (2016) 2087.
16. A.K. Chandrappa, L.R. Potnuru and P.C. Ramamurthy, *J. Alloy. Compd.*, 745 (2018) 555.
17. C. Tealdi, L. Malavasi, I. Uda, C. Ferrara, V. Berbenni and P. Mustarelli, *Chem. Commun.*, 50 (2014) 14732.
18. J. Xu, X. Wang, H. Fu, C.M. Brown, X. Jing, F. Liao, F. Lu, X. Li, X. Kuang and M. Wu, *Inorg. Chem.*, 53 (2014) 6962.
19. Y. Jee, X. Zhao and K. Huang, *Chem. Commun.*, 51(2015) 9640.
20. K.K. Inglis, J.P. Corley, P. Florian, J. Cabana, R.D. Bayliss and F. Blanc, *Chem. Mater.*, 28 (2016) 3850.
21. P.-H. Chien, Y. Jee, C. Huang, R. Dervisoglu, I. Hung, Z. Gan, K. Huang and Y.-Y. Hu, *Chem. Sci.*, 7 (2016) 3667.
22. A. Pandey, U.K. Chanda, L. Besra, K.K. Sahu, A. Roy and S. Pati, *J. Electroceram.*, 40(2017) 50.
23. R. Pandey, M. Viviani, P. Singh, R. Botter, M.P. Carpanese, A. Barbucci and S. Presto, *Solid State Ionics*, 314 (2018) 172.
24. R.D. Shannon, *Acta Cryst.*, A32 (1976) 751.